EAN 2012
50th annual coference on experimental stress analysis

STRESS ANALYSIS OF AN INDUSTRY HALL'S DEEP BEAM

Diana Šimić[1], Ana Grubešić[2]

Abstract: The stress and strain analysis for a complexly-shaped deep beam to be used in an industrial hall building was conducted theoretically, through finite element method, and experimentally, by deep beam model testing in laboratory. The laboratory tested model of a deep beam was made of a medium density fibreboard (MDF) plate, 38 mm in thickness. Mechanical characteristics of the medium density fibreboard were determined by laboratory testing of fibreboard specimens. During the deep beam model testing in laboratory, characteristic cross sections were subjected to strain measurements by means of resistance strain gauges, while inductive gauges were used for measuring displacements. In the course of laboratory testing, the load applied on the deep beam model was gradually increased in four phases. The relaxation of load between individual loading phases, was followed by an increased application of load. After results obtained by model testing in laboratory were analyzed and compared with those obtained by the finite element method, it was established that a good correspondence of results was obtained during the stress and strain analysis of deep beams.

Keywords: deep beam, stress, strain, strain gauges, finite element method (FEM), mechanical properties, medium density fibreboard

1. Introduction

A complexly shaped deep beam for an industrial hall was subjected to horizontal loading, as shown in Figure 1. The stress and strain analysis for the deep beam was conducted theoretically, using the finite element method (FEM) [1-5], and experimentally [6-10], by model testing in laboratory. The deep beam model is made of a medium density fibreboard 38 mm in thickness, Figure 1.

MDF is medium density fiber wood. It was created smashing hard and soft wood types as well as mixing and combining it with a binders such as resins and waxes [11]. Finite element method (FEM) [4,5] is significant support in the engineering analysis. The method was designed in the fifties of the twentieth century, since when has a wide application in engineering. Finite element method (FEM) is a numerical method for solving a set of related equations obtained by approximating the area of continuous variables in the final set of variables, the number of discrete points (nodes) of the field.

[1] *Prof. Diana Šimić, Ph.D.; University of Zagreb Faculty of Civil Engineering; fra Andrije Kačića Miošića 26,10000 Zagreb,Croatia;dianas@grad.hr*

[2] *Ana Grubešić, MEng.; University of Zagreb Faculty of Civil Engineering; fra Andrije Kačića Miošića 26,10000 Zagreb,Croatia*

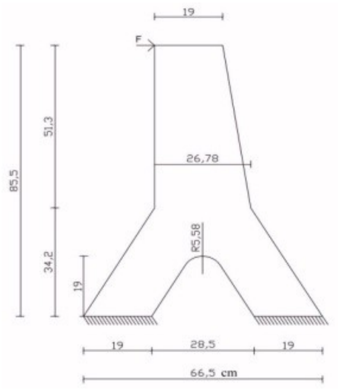

Fig. 1. Deep beam model

2. Determining mechanical properties of medium density fibreboards

Mechanical properties of medium density fibreboards [11] were determined prior to the deep beam model testing. Medium density fibreboard specimens were tested in ZWICK apparatus. Z600E is a universal electrically-operated compression/tension testing machine, 600 kN in capacity. It ranks among the most modern and highly accurate laboratory testing machines. The tensile strength of medium density fibreboards was determined by subjecting specimens measuring d/b/h = 38/3.8/3.8 cm [6-9] to bending load, Figure 2.

The compressive strength [6-9] of a medium density fibreboard [11] plate subjected to load parallel to fibres was determined on prismatic specimens measuring d/b/h=7.6/3.8/7.6 cm, Figure 3.

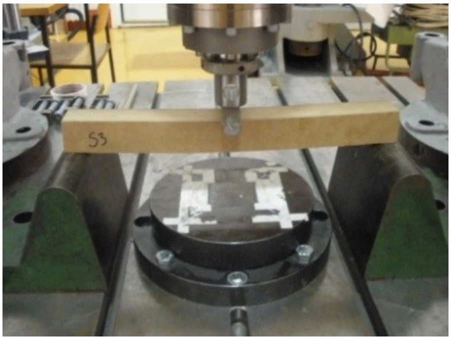

Fig. 2. Medium density fibreboard specimen subjected to flexural strength testing

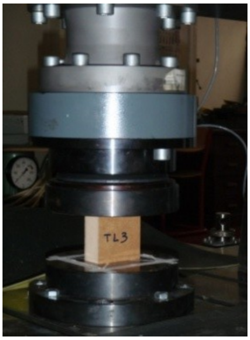

Fig. 3. Specimen subjected to compressive load parallel to fibres

The tensile strength data for a medium density fibreboard specimen subjected to flexural strength testing, in the direction parallel to fibres, are presented in Table 1.

Table 1. Tensile strength of a medium density fibreboard specimen subjected to flexural strength testing parallel to fibres

	Specimen 1	*Specimen 2*	*Specimen 3*
F_{max} [kN]	2.55	2.48	2.62
σ_M [MPa]	26.45	25.72	27.26
$\sigma_{M, avg}$		26.48	

The data on compressive strength of a medium density fibreboard subjected to load parallel to fibres are shown in Table 2.

Table 2. Compressive strength of medium density fibreboard specimens subjected to compressive load parallel to fibres

	Specimen 1	*Specimen 2*	*Specimen 3*
F_{max} [kN]	43.82	42.76	45.99
σ_{TL} [MPa]	15.57	14.81	15.93
$\sigma_{TL, avg}$		15.30	

Strain diagrams for specimens 1, 2, 3 with load applied parallel to fibres are presented in Figure 4. The strain diagram for specimens 1, 2, 3 at compressive load parallel to fibres is shown in Figure 5.

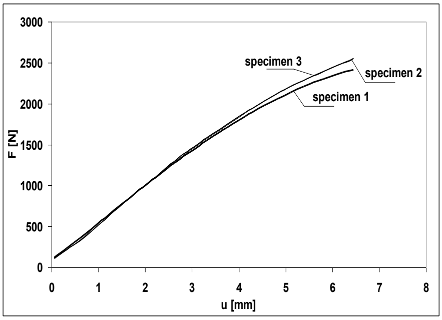

Fig. 4. Strain diagram for specimens 1, 2, 3, with load applied parallel to fibres

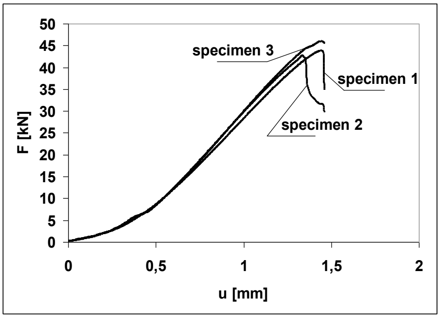

Fig. 5. Strain diagram for specimens 1, 2, 3 at compressive load parallel to fibres

Elastic constants for the medium density fibreboard, i.e. elastic modulus E and Poisson ratio ν [6-10], were determined on three prismatic specimens measuring d/b/h=7.6/3.8/22.8 cm at compressive load parallel to fibres. The strain was measured on prismatic specimens using resistance strain gauges. Four resistance strain gauges were attached to the specimen: at the front side, parallel to fibres T_1 and perpendicular to fibres T_2 and, at the back side, parallel to fibres T_4 and perpendicular to fibres T_3, Figure 6, 7.

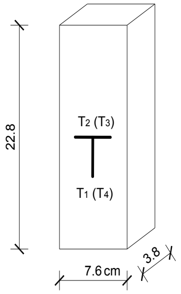

Fig. 6. Medium density fibreboard specimens with resistance strain gauges in position

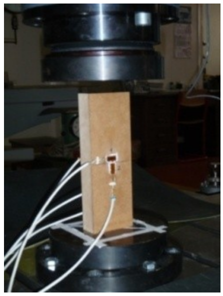

Fig. 7. Specimen in testing machine during compressive strength testing parallel to fibres

The medium density fibreboard specimens were tested in three loading and unloading cycles. Test results were used to calculate mean values of the modulus of elasticity $\bar{E}^{"} = 2900MPa$ and Poisson ratio $\bar{\nu}$=0.32.

3. Testing thin-walled beam model in laboratory

The thin walled beam model is a single piece element made of a medium-density fibreboard plate 38 mm in thickness, Figure 1. During the loading action, the strain and displacement measurement was conducted in three typical cross-sections. The arrangement of measurement points along the model is shown in Figure 8.

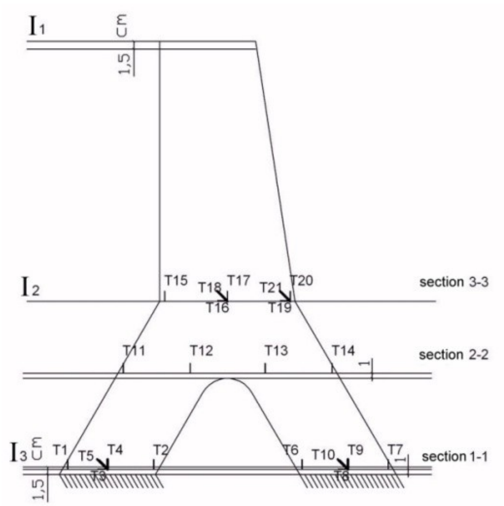

Fig. 8. Arrangement of resistance strain gauges "T" used for strain measurement, and inductive gauges "I" for measuring thin-walled beam displacements

The model with resistance strain gauges for strain measurement, and inductive gauges for displacement measurement, ready for testing [6-10], is shown in Figure 9.

Fig. 9. Model with resistance strain gauges and inductive gauges, ready for testing

Fig. 10. View of deep beam failure

The deep beam model testing [6-10] was conducted in four loading phases, and the loads were applied as follows: F_1=2.5 kN; F_2=5.0 kN; F_3=7.5 kN i F_4=10.0 kN. Each phase was followed by relaxation of load (unloading), and then by a new application of load. The load was applied using a hand-operated Holmatro compression machine. In the course of this loading, the stress values did not exceed limit stresses that were obtained during the bending test. The model failure occurred at the force of F = 11.0 kN, Figure 10. At measurement points T_1, T_2, T_6, T_7, T_{11}, T_{12}, T_{13}, T_{14} i T_{15} strains were measured in one direction only. Stresses are determined by the following expression: $\sigma = \varepsilon \cdot E$. Four type K rosettes were placed on the model, Figure 11. The rosette R_1 is formed of strain gauges T_3, T_4, T_5, the rosette R_2 is formed of strain gauges T_8, T_9, T_{10}, the rosette R_3 is formed of strain gauges T_{16}, T_{17}, T_{18}, and the rosette R_4 is formed of strain gauges T_{19}, T_{20}, T_{21}.

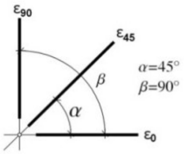

Fig. 11. K-rosette

The value of principal strain is defined by the expression:

$$\varepsilon_{1,2} = \frac{\varepsilon_0+\varepsilon_{90}}{2} \pm \frac{\sqrt{2}}{2} \cdot \sqrt{(\varepsilon_0 - \varepsilon_{45})^2 + (\varepsilon_{45} - \varepsilon_{90})^2}, \tag{1}$$

and the direction of principal strains is defined by the expression:

$$tg2\varphi = \frac{2\varepsilon_{45}-\varepsilon_0-\varepsilon_{90}}{\varepsilon_0-\varepsilon_{90}}. \tag{2}$$

Principal stresses are defined by the expression:

$$\sigma_{1,2} = \frac{E}{1-\nu} \cdot \frac{\varepsilon_0+\varepsilon_{90}}{2} \pm \frac{E}{\sqrt{2}(1+\nu)} \cdot \sqrt{(\varepsilon_0 - \varepsilon_{45})^2 + (\varepsilon_{45} - \varepsilon_{90})^2} \tag{3}$$

Stresses in the direction of measured strains are defined by the following expressions:

$$\sigma_X = \frac{\sigma_1+\sigma_2}{2} + \frac{\sigma_1-\sigma_2}{2} cos2\varphi \tag{4}$$

$$\sigma_y = \frac{\sigma_1+\sigma_2}{2} - \frac{\sigma_1-\sigma_2}{2} cos2\varphi \tag{5}$$

$$\tau_{xy} = \tau_{yx} = \frac{\sigma_1-\sigma_2}{2} sin2\varphi \tag{6}$$

The stresses σ_x, σ_y, τ_{xy} (x axis is in the cross-sectional plane, while y axis is perpendicular to the cross-sectional plane) were determined using the previously established elastic modulus E=2900 MPa and Poisson ratio ν=0.32 values, and making use of expressions (1)-(6) at rosette measurement points. Stresses for all four loading phases are presented in Table 3. Table 4 shows displacements in measurement points I_1, I_2, I_3 for all four loading phases.

4. Deep beam analysis model

The deep beam model was analyzed using the finite element method and the program package SAP 2000 [1-5]. The finite element network is presented in Figure 12. The following mechanical properties of the medium density fibreboards are defined in the model: elastic modulus E = 2900 MPa and Poisson ratio ν=0.32. The model analysis was conducted for four loading phases, which correspond to model load phases used during model testing in laboratory.

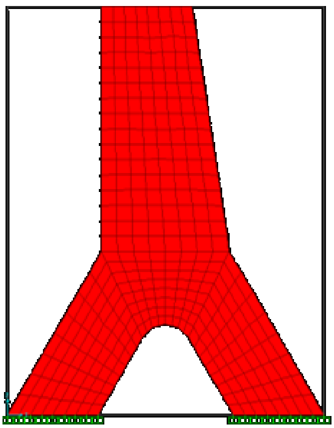

Fig. 12. Finite element network

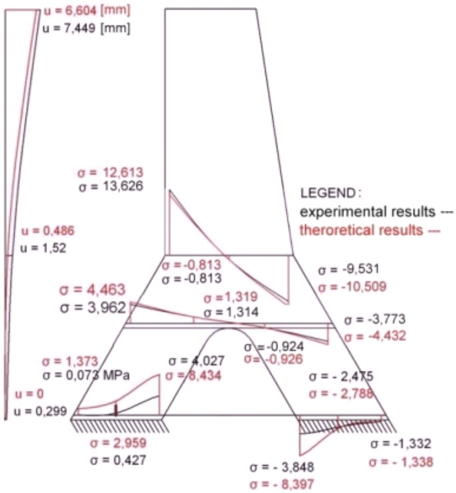

Fig. 13. Stress and displacement diagrams

5. Comparison of results in measurement points as obtained by model analysis and during testing

The comparison of stress results for all four loading phases is presented in Table 3, while comparison of displacement results is shown in Table 4. The graphical comparison of stress and displacement results in the fourth model loading phase (F=10 kN) is presented in Figure 13.

Table 3. Comparison of stress results for four loading phases

Stress [MPa]			F=2.5 kN		F=5.0 kN		F=7.5 kN		F=10.0 kN	
			Testing	Analysis	Testing	Analysis	Testing	Analysis	Testing	Analysis
T1		σ_y	0.017	0.328	0.038	0.667	0.053	1.012	0.073	1.373
T2		σ_y	0.911	2.134	1.990	4.169	3.045	6.268	4.027	8.434
T3	R1	σ_x	0.160	0.235	0.147	0.457	1.800	0.706	2.491	0.942
T4		σ_y	0.514	0.694	0.318	1.446	0.391	2.219	0.427	2.959
T5		τ_{xy}	0.117	0.117	0.240	0.228	0.332	0.332	0.430	0.432
T6		σ_y	-0.892	-2.103	-1.733	-4.101	-2.675	-6.101	-3.848	-8.397
T7		σ_y	-0.429	-0.342	-0.935	-0.671	-1.188	-1.011	-1.332	-1.338
T8	R2	σ_x	-0.302	-0.302	-0.255	-0.470	-1.068	-0.605	-1.287	-0.901
T9		σ_y	-0.575	-0.575	-1.543	-1.425	-1.874	-2.101	-2.475	-2.788
T10		τ_{xy}	0.113	0.113	0.278	0.260	0.358	0.354	0.450	0.463
T11		σ_y	0.964	1.130	1.979	2.223	2.961	3.410	3.962	4.463
T12		σ_y	0.271	0.272	0.603	0.603	0.949	0.949	1.314	1.319
T13		σ_y	-0.227	-0.272	-0.426	-0.426	-0.658	-0.657	-0.924	-0.926
T14		σ_y	-0.952	-1.091	-1.896	-2.042	-2.809	-3.203	-3.773	-4.432
T15		σ_y	3.023	3.181	6.204	6.204	9.603	9.529	13.626	12.613
T16	R3	σ_x	0.008	0.007	0.156	0.155	0.015	0.012	0.283	0.278
T17		σ_y	-0.146	-0.146	-0.413	-0.403	-0.402	-0.404	-0.813	-0.813
T18		τ_{xy}	0.077	0.076	0.235	0.110	0.152	0.131	0.352	0.153
T19	R4	σ_x	-0.618	-0.603	-1.235	-1.223	-1.854	-1.835	-2.546	-2.454
T20		σ_y	-2.316	-2.714	-4.624	-5.374	-6.958	-7.674	-9.531	-10.509
T21		τ_{xy}	0.510	0.642	1.011	1.446	1.519	2.420	2.075	3.142

Table 4. Comparison of displacement results for four loading phases

Displacements [mm]	F=2.5 kN		F=5.0 kN		F=7.5 kN		F=10.0 kN	
	Testing	Analysis	Testing	Analysis	Testing	Analysis	Testing	Analysis
I1	1.135	1.663	2.985	3.302	4.858	4.935	7.449	6.604
I2	0.200	0.123	0.450	0.243	0.845	0.365	1.520	0.486
I3	0.014	0.000	0.040	0.000	0.102	0.000	0.299	0.000

The load-stress diagram for the measurement point T_{15}, obtained by model testing for all four loading phases, is shown in Figure 14. The load-displacement diagram for the measurement point I_1, obtained by model testing for all four loading phases, is shown in Figure 15.

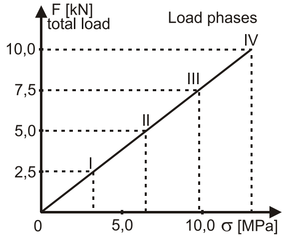

Fig. 14. Load-stress diagram at measurement point T_{15}

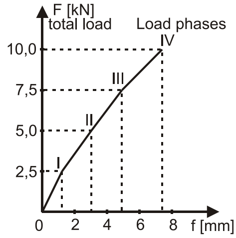

Fig. 15. Load-displacement diagram at measurement point I_1

6. Conclusion

The deep beam model testing was conducted in four loading phases, and the load was increased in each subsequent phase. The linear dependence for load – stress, and an approximately linear dependence for load - displacement, was obtained for all four phases through laboratory testing. After results obtained by deep beam model testing in laboratory were analyzed and compared with those obtained by model analysis, a good correspondence of theoretical and experimental results was established for stresses and displacements.

References

[1] Zienkiewicz O. C., *The Finite Element Method in Structural and Continuum Mechanics* (McGraw-Hill, London, 1970).

[2] ..., *Sap 2000 Analysis Reference Manual* (Computers and Structures, Inc., Berkeley, 2002).

[3] Schueller W., Building *Support Structures: Analysis and Design with SAP2000 Software* (Computer and Structures Inc., Berkeley, 2008). 0923907750.

[4] Wriggers P., *Finite Elemente in der Baupraxis* (Ernest & Sohn, Darmstadt,1988). 3433017751.

[5] Huebner K. H., Dewhirst D. L., Smith D. E., Byrom T. G., *The finite element method for engineers* (John Wiley & Sons, Canada, New York, 2001). 0471370789

[6] Dally J. W, Riley W. F., *Experimental Stress Analysis* (McGraw-Hill, New York, 1991). 0070152187

[7] Holman J. P., *Experimental Methods for Engineers* (McGraw-Hill, New York, 1994). 0070296669

[8] Luzhin V., Zlochevsky A. B., Gorbunov A., Volohov V. A., *Inspection and Testing of Civil Engineering Structures*, (Mir Publisher, Moscow, 1987).

[9] Kobayashi A. S., *Handbook on Experimental Mechanics* (Prentice-Hall, New Jersey, 1990). 0133777065

[10] Montero W., Farag R., Diaz V., Ramirez M., Boada B. L., "Uncertainties Associated with Strain Maeasuring Systems Using Resistance Strain Gauges", *The Journal of Strain Analysis for Engineering Design*, **46** (1), pp. 1-13 (2011). 0309-3247

[11] Ganev S., Gendron G., Cloutier A., "Beauregard R., Mechanical Properties of MDF as a Function of Density and Moisture Content", *Wood and Fiber Science*, **37** (2), pp 314–326 (2005). 0735-6161